Planar Lipid Bilayers as Light Guides

H. P. Braun, R. Herrmann, and M. E. Michel-Beyerle
Institut für Physikalische und Theoretische Chemie, Technische Universität München

Z. Naturforsch. **34a**, 1436–1445 (1979); received October 29, 1979

The light guide properties of planar lipid bilayers are discussed and experimentally verified. The interaction between the light and the constituents of the bilayer is substantially increased since the light path is as large as the diameter of the film, e.g. of the order of several millimeters. The influence of electric fields on the bilayer and on the bilayer-torus transition region has been investigated. Field induced generation of scattering centers is detected in solvent containing bilayers.

Introduction

In the past planar lipid bilayers [1] have attracted interest with respect to their model character for the lipoidal element in cell membranes. Information on the permeability and the selectivity of ion transport across the bilayer has been derived from steady state current-voltage characteristics, and information on the bilayer thickness and its dielectric properties from the capacitance [2]. The dynamics of molecular constituents of the bilayer were approached via time resolved capacitance [3] and charge pulse [4] measurements.

Optical and spectroscopic techniques in normal incidence are standard tools in black film research though the minute amount of material incorporated in bilayers produces only weak effects on the probing light. Thus, interferometric techniques suffer from the short path of interaction of some ten Angströms within the bilayer which is exceeded by many orders of magnitude by the path of the probing light through the adjacent electrolytes. Due to the phase noise generated in the electrolyte, interferometric methods are limited to those parts of the film which are comparable to the wavelength of the probing light, like the torus-bilayer region and lenses [5].

In this paper we present the basic concept of an optical technique [6] based on a strongly increased light path within the bilayer. This method seems to be appropriate for the resolution of bilayer dynamics such as thermally induced changes including phase transitions, dielectric relaxation, conformational changes induced by external parameters (e.g. electric field, pressure) and lateral motion of membrane constituents (e.g. built-in proteins, chromophors).

The technique is based on the light guiding properties of planar lipid films. It profits from the long path of interaction between the light and the film given by the diameter of the aperture. Along this path the microscopic effects are summed up yielding information on electric relaxation processes and conformational changes within the bilayer. The method is suited for scattering and absorption experiments since a high intensity wave travels along the film. The light is guided along the bilayer even through curvatures. Thus, the volume of interaction is always properly defined, and there is no need for difficult optical alignment. The method reveals the lateral optical properties of the planar film and is therefore expected to contribute to the knowledge of the anisotropic properties of lipid bilayers. The technique is, in principle, applicable to any film with a refractive index higher than the one of the adjacent medium including solvent free bilayers [7, 8] and also thick polymer films.

In the following, the light guide properties of the lipid bilayer and the corresponding light coupling technique by optical fibers are discussed and experimentally verified. The power of the method is illustrated by the influence of an electric field on the shape and structure of a solvent-containing lipid film.

Reprint requests to Dr. H. P. Braun or Dr. M. E. Michel-Beyerle, Institut für Physikalische und Theoretische Chemie, Technische Universität München, Lichtenbergstr. 4, D-8046 Garching.

Theoretical Considerations

Wave Guide Properties of a Planar Lipid Bilayer

Figure 1 shows a scheme of the light guide. The bilayer with a thickness $2d$ and an index of refrac-

0340-4811 / 79 / 1200-1436 $ 01.00/0. — Please order a reprint rather than making your own copy.

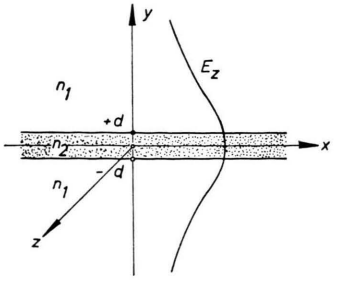

Fig. 1. Scheme of a planar light guide. n_1: index of refraction of the electrolyte, n_2: index of refraction of the bilayer, d: half thickness of the bilayer.

tion n_2 is immersed in an aqueous electrolyte with index n_1, infinitely extending to both sides. In a simplified treatment it is assumed that both, bilayer and electrolyte are isotropic loss free media. The solutions of the Maxwell equations for the geometry represented in Fig. 1 have been worked out in optical notation [9].

The discussion will be restricted to the transversal electric (TE) wave; similar expressions are valid for the transversal magnetic polarization. The non-zero components of the TE-wave are:

$$E_z; H_x = \frac{1}{i k_0} \frac{\partial E_z}{\partial y}; \quad H_y = \frac{1}{i k_0} \frac{\partial E_z}{\partial x}; \quad (1)$$

k_0 denotes the wave vector of the light with a vacuum wavelength λ_0. The relation between the wave vectors and indices of refraction of the corresponding media is given by (2) where the index j stands for the media: vacuum = 0, electrolyte = 1 and bilayer = 2.

$$k_j = 2\pi n_j/\lambda_j . \quad (2)$$

The field distribution inside the bilayer is given by

$$E_{z(\text{inside})} = A_i \exp(i\alpha x) \cos[(k_2^2 - \alpha^2)^{1/2} y] \quad (3)$$

with $Y \leqq d$, and the outside field is an exponentially attenuated continuation of the center wave.

$$E_{z(\text{outside})} = A_0 \exp(i\alpha x - \beta y) . \quad (4)$$

with $y \geqq d$. The amplitudes A_i and A_0, the propagation constant α and the attenuation factor β are determined by satisfying the continuity conditions for tangential E_z and H_x at the interface $y = \pm d$.

The relation between the amplitudes A_0 and A_i is derived from the continuity of E_z

$$A_0 = A_i \exp(+\beta d) \cdot \cos[(k_2^2 - \alpha^2)^{1/2} d] \quad (5)$$

whereas the continuity of H_x determines the propagation constant α and the attenuation factor β.

$$(k_2^2 - \alpha^2) \tan[(k_2^2 - \alpha^2)^{1/2} d] - (\alpha^2 - k_2^2)^{1/2} = 0 . \quad (6)$$

Equation (6) is transcendental and cannot directly be solved for α. Instead of dealing with the vectors k_j, (6) can be rearranged using the optical notation [9]. An index of refraction N is attributed to the wave guide system assigning a common phase velocity to the inner and outer wave:

$$\alpha = k_0 N , \quad (7)$$

$$d/\lambda_0 = (2\pi)^{-1} \cdot (n_2^2 - N^2)^{-1/2} \cdot \tan^{-1}\{(N^2 - n_1^2)^{1/2}/(n_2^2 - N^2)^{1/2}\}. \quad (8)$$

Whenever N is determined by a numerical approximation or graphical solution the attenuation factor β can be calculated from

$$\beta = (2\pi/\lambda_0)(N^2 - n^2)^{1/2} . \quad (9)$$

An examination of (8) is leading to the following conclusions:

Since d/λ_0 is real, the right hand side of (8) must also be real which implies that the index of refraction of the lipid material n_2 must be higher than that of the adjacent electrolyte n_1. This is the prerequesite for a dielectric waveguide.

As a consequence of the small d/λ_0 ratio for visible light ($\cong 10^{-2}$), the index of refraction N of the system is close to n_1.

The choice of the cosine distribution in (3) is justified by the even symmetry with respect to the plane $y = 0$, because there is no cut-off if d approaches zero. In the case $d = 0$ an unbond plane wave with amplitude A_i propagates along $y = 0$. Odd modes having a sine distribution cannot propagate for vanishing d.

A further consequence of the small d/λ_0 ratio is that the tangent in (8) has a single value implying that only waves of zero mode can propagate and the mode indices can be omitted.

Figure 2 shows a plot of numerical solutions of (8) depicting the relation between the reduced thickness of the bilayer ($2d/\lambda_0$) and the index of refraction N of the wave guide system. The index of refraction n_1 of the electrolyte ($n_1 = 1.34$ corresponding to 10^{-3} M KCl in water) is kept constant whereas the index n_2 of the bilayer material varies from 1.35 to 1.6. The attenuation factors β given in

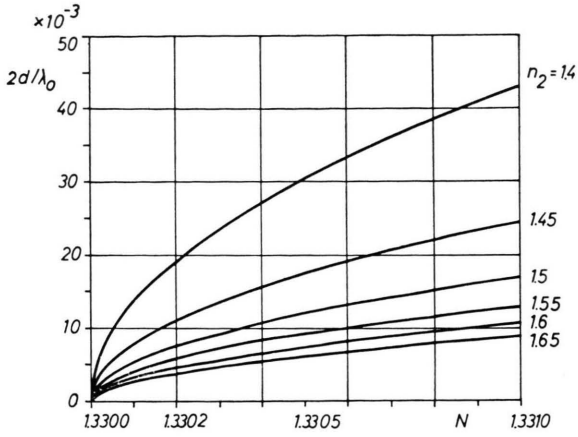

Fig. 2. Relation between the reduced thickness $2d/\lambda_0$ and the index of refraction N for a TE_0 mode wave guide with the geometry depicted in Figure 1. The index of refraction of the electrolyte $n_1 = 1.34$ is kept constant, the index of the lipid material ranges from 1.4 to 1.65.

Table 1. Lateral attenuation factors β for light (5000 Å) propagating along a wave guide of 50 Å thickness. The results are calculated with Eq. (9) using the parameters given in Figure 2.

n_2	N	β [Å^{-1}]
1.40	1.34001	$6.50 \cdot 10^{-}$r
1.45	1.34004	$1.21 \cdot 10^{-5}$
1.50	1.34008	$1.79 \cdot 10^{-5}$
1.55	1.34014	$2.39 \cdot 10^{-5}$
1.60	1.34020	$2.96 \cdot 10^{-5}$

Table 1 are computed for a typical bilayer thickness of $2d = 50$ Å. The wavelength of the guided light is 5000 Å.

Generally the indices of refraction are complex whereupon the propagation constant α turns also out to be complex. This indicates absorption losses and generates radiative modes escaping from the wave guide. For small losses the guiding properties are still maintained as has been shown by perturbation analysis [9, 10]. This effect can be used to perform optical absorption experiments on built-in chromophors. In contrast to normal incidence experiments, the absorption following Lambert-Beers law is considerably enhanced [10, 11]. In the following this sensitivity gain will be calculated by comparing the ratios of the total power dissipated by the absorbing species and the light power flowing through the sample for the two cases, normal incidence and the wave guide mode.

A layer of unit area is considered containing M molecules with an absorption coefficient σ. The exponential decay of the light power along the light path is neglected for a sufficiently small product $M\sigma$. The power absorbed per unit length is

$$P_{\text{abs}} = M \sigma p \tag{10}$$

where $p = n_2^2 E^2/(8\pi)$ is the power density. The power flow is calculated from the x-component of the Poynting vector:

$$P_{\text{flow}} = \frac{c}{8\pi} \operatorname{Re}(E_z \times H_y^*) \tag{11}$$

(c: velocity of light).

In the normal incidence case, a plane wave with TE-polarization is assumed to propagate througth the sample area. Then the ratio $P_{\text{abs}}/P_{\text{flow}}$ is simply given by

$$(P_{\text{abs}}/P_{\text{flow}})_{\text{normal incidence}} = M \sigma n_2/(2c) . \tag{12}$$

The power density in the center of the wave guide at the position of the absorbing molecules ($y = 0$) can be calculated by squaring (5). The absorbed power in the waveguide is then

$$P_{\text{abs}} = MN^2 \sigma A_i^2/(8\pi) . \tag{13}$$

In order to calculate the power flow carried by the center and surface waves one makes use of the symmetry of the wave guide with respect to the plane $y = 0$. The integral for a TE-wave according to (11) is split into two parts:

$$P_{\text{flow}} = \frac{cN}{4\pi} \left[\int_0^d E_{z(\text{inside})}^2 \, dy + \int_d^\infty E_{z(\text{outside})}^2 \, dy \right] . \tag{14}$$

A good approximation for the integral in (14) is

$$P_{\text{flow}} = \frac{cN}{4\pi} A_i^2 \left(d + \frac{1}{2\beta} \right) \tag{15}$$

since the field amplitude A_i within the bilayer is almost constant. The thickness can also be neglected when compared to the reciprocal of 2β. As shown in the Table 1 $(2\beta)^{-1}$ exceeds d by three orders of magnitude. Thus, the reciprocal of the attenuation constant of the surface wave determines the effective thickness of the wave guide and its cross sectional intensity profile. The absorption ratio for the wave guide is

$$P_{\text{abs}}/P_{\text{flow}} = M \sigma N (2c)^{-1} [d + 1/(2\beta)]^{-1} , \tag{16}$$

and the sensitivity enhancement Q is given by

$$Q = (P_{\text{abs}}/P_{\text{flow}})_{\substack{\text{wave}\\ \text{guide}}}/(P_{\text{abs}}/P_{\text{flow}})_{\substack{\text{normal}\\ \text{incidence}}}$$
$$= 2N\beta/n_2 . \quad (17)$$

This result can be explained geometrically, saying that one linear dimension of the layer area exposed to the light flux in normal incidence is reduced to the effective thickness of the wave guide $d_{\text{eff}} = (2\beta)^{-1}$ while the number of absorbing molecules remains constant. This is equivalent to an effective increase of the density of absorbers; e.g. the absorption measured in normal incidence of a layer of 1 cm² is enhanced by a factor of 3000 upon applying the light guide technique with the data given in the Table 1 ($n_2 = 1.5$).

Light Coupling Properties of the Plateau-Gibbs Border

The probing light is fed to and collected from the film by means of optical fibers being immersed into the torus volume. Two coupling processes take place within the torus; at the input side there is the coupling of light from the glass fiber to the torus which then couples the light to the bimolecular area. At the output side the identical process takes place in reversed succession. The coupling processes are discussed with respect to the coupling efficiency which is defined by the ratio of power transmitted to the bilayer versus output power from the glass fiber.

Only one of the coupling processes at the entrance or the exit needs to be investigated, since the reciprocity allows to interchange the source with the observer. The coupling efficiency is exclusively dependent on the shape of the Plateau-Gibbs border. Its geometry has been calculated by minimizing its surface free energy at equilibrium which is equivalent to calculating the minimum surface area for a given torus volume [12]. The shape is determined by the contact angle γ of the thin film with the torus transition region and the contact angle δ of the torus separator interface. Figure 3 shows a cross sectional view of the lipid membrane system with input and output fibers immersed in the torus. The contour of the torus is similar to a horn shaped coupler of which the coupling efficiencies have been investigated for integrated optics applications [13, 14]. The incident wave from the bilayer generates a reflected and a transmitted wave, which are both

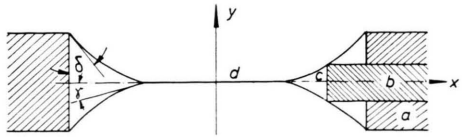

Fig. 3. Cross sectional view of a lipid membrane. a: separator foil, b: glass fiber, c: torus volume, d: bimolecular area, γ: contact angle between torus and bilayer, δ: contact angle between torus and separator.

accompanied by radiating waves contributing to the radiation losses of the coupler. It is impossible to obtain exact solutions for this problem. Therefore the contour of an individual coupler is approximated by a series of abrupt steps of infinitesimal height neglecting the reflection and the radiation losses. Theory predicts high coupling efficiencies close to 1 for tapered couplers as long as their thickness reduces gradually within hundreds of wavelength from its initial thickness to $\lambda/2$ [13]. Thus, for the first step in coupling between the optical fiber and the torus volume a coupling efficiency close to 1 can be assumed, since the thickness of the torus reduces gradually within the limits mentioned above. The coupling efficiency is predominantly governed by the torus bilayer transition region which is defined by a decrease in thickness from 5000 Å to the bimolecular dimensions of about 50 Å [12]. The length of the transition region depends on the contact angle γ. For most of the lipids used γ ranges from 2° to 8° [5] and the length of the transition zone is less than 10 μm [12]. Thus the radiation loss of this transition region is considerable since the thickness decreases by a factor of 50 along a light path which is shorter than 20 wavelengths. Therefore according to [13] coupling efficiencies of the order of 10^{-3} are to be expected for either the entrance or the excit coupling, yielding a total coupling efficiency of 10^{-6} for the lipid film between the two fiber ends.

Experimental Details

Separator Foil and Optical Fibers

The bilayers are prepared according to standard techniques [1]. A solution of lecithine in decane is spread over a circular hole in an electrically insulating foil which separates two electrolyte compartments. Then the bimolecular film develops by expelling the solvent. The separator foil is made from two sheets of thermally welded polyethylene

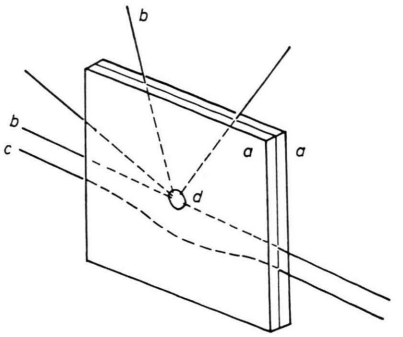

Fig. 4. Separator foil. a: Two 0.05 mm foils of polyethylene, thermally welded with surfaces hydrophobized with silicone, b: multimode glass fiber with 40 μm diameter and a numerical aperture of 0.17, c: reference fiber, d: film aperture (2 mm).

with glass fibers sandwiched in between (Figure 4). In order to shorten the light path through the non-bimolecular region of the lipid film, the hydrophobized ends of the fibers extend into the torus volume without affecting the stability of the membrane.

The optimum coupling efficiency for the fiber-torus interface can be obtained when light of zero mode is fed into the torus; this requires single-mode fibers or controlled mode launching into multimode fibers. Properly defined modes can be excited in a fiber by generating the appropriate radiation pattern of the mode at the input side of the fiber [15]. The glass fibers used in the experiment are multimode fibers which have been modified to support only zero modes. The reflective coating of the fibers has been removed for about 1 cm length, and the fiber core is immersed in a material with index of refraction greater than that of the core. Thus, the conditions for total reflection being violated, high order modes radiate off, whereas the zero modes guided in parallel to the fiber axis are less attenuated. The degree of zero mode selection can be monitored by measuring the angle of aperture of the light cone at the output side of the fiber which is 0.4° for the fiber used. Perfect circular shaped fibers with a stress-free core maintain the direction of polarization for the zero modes which makes this type of fibers best suited for polarization experiments. Since this mode filtering technique described is inflicted with high losses care must be taken to excite predominantly the lowest modes. Otherwise, with uniform excitation of all modes the power would be distributed to about 1000 higher modes which are excitable in the type of fibers used.

The experimental setup is depicted in Figure 5. Light of 4579 Å wavelength from an krypton laser (Spectra Physics 164) is focussed with a lens of 300 mm focal length into the fiber. The fibers are 150 mm long; mode filtering is done immediately before the fiber enters the separator foil. The light transmitted by the membrane is fed into a similarly prepared fiber and analyzed with a polarizer before being detected with a photomultiplier (RCA 1P28). The dc-component of the photocurrent is measured with an electrometer (Keithley 610B) and recorded. Photocurrent transients are processed with a Tektronix WP 2221 system. The bilayer can be excited with square-wave voltage pulses from a DDD pulser (model 5109, Electronic Counters Inc.); its capacitance is measured with a Thompson-type capacitance bridge. Provisions are made to manipulate the area of the lipid film via bulging by controlling the electrolyte levels with a micrometer driven bar dipping into one of the two compartments.

Preparation of the Bilayer

The lipid film is prepared over a hole with an aperture of 2 mm. 1,2-Di-isostearoyl-3-sn-phosphtidylcholine (DISL) was used as lipid. Its physical, optical and electrical properties are described in detail in [16]. The index of refraction

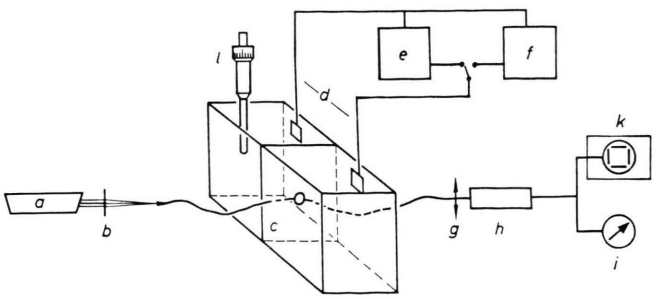

Fig. 5. Experimental arrangement. a: laser, b: lenses, c: separator, d: electrodes, e: capacitance bridge, f: pulse generator, g: polarizer, h: photomultiplier, i: current meter, k: transient digitizer, l: micrometer screw for adjustment of the electrolyte level.

n_2 of a 2% DISL-solution in *n*-decane is 1.4, the index n_1 of the $5 \cdot 10^{-3}$ M KCl aqueous electrolyte used was 1.34.

Results and Discussion

Proof of Light Guide Effect

In order to make use of the light guide properties of the lipid film, the ratio between the light intensities guided and directly transmitted between the fibers is important since the stray intensity may compete or even cover the guided light intensity. In the absence of a lipid film an unbound linearly polarized wave is transmitted which determines the maximum background of stray light. By optically linking the fibers with a plane lipid film the transmitted intensity is expected to change depending on the coupling and light guiding properties of the film.

The light guiding properties of the lipid film are put to test in an arrangement allowing to guide the light around a curvature, thus avoiding a direct view between the fiber ends. This is experimentally verified (Fig. 6a) by bulging the foil near the film aperture towards one side. This way the radiation cones of the fibers are directed some degrees out of the plane of the separator foil. To ensure proper coupling conditions, the lipid film is spherically bulged to this side until the surface tangents of the film in the transition region coincide with the axis of the glass fibers. The film can be bulged by applying hydrostatic pressure from the opposite side.

The degree of film bulging is monitored by the electrical capacitance with the assumption that an increase in the capacitance is proportional to the bimolecular area. Figure 6b shows the transmitted intensity as a function of the capacitance of the bulged film and of the angle θ. This is the angle between the plane film at minimum capacitance and the surface tangent of the bulged film in the transition region near the rim of the aperture. The relative change of the capacitance as a function of the angle θ is given by the equation

$$C(\theta)/C_0 = 2\,(\cos\theta - 1)/\sin^2\theta\,, \qquad (18)$$

derived for the geometry shown in the scheme of Figure 6a. There is a distinct maximum of transmission if θ is equal to the cone angle of the fibers

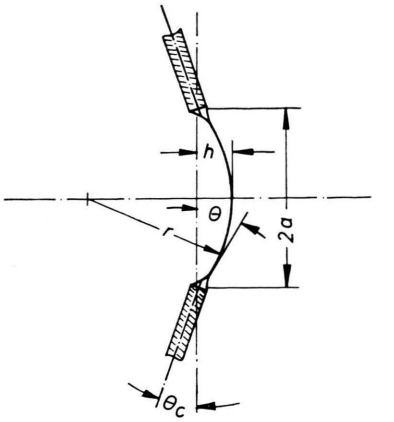

Fig. 6a. Scheme of a bulged film. $2a$: diameter of the film aperture, r: bending radius of the bulged film, h: height of the sphere, θ: angle of the surface tangents of the bulged film at the rim of the aperture with the plane film at minimum capacitance, θ_c: angle of the fiber axis with the separator foil.

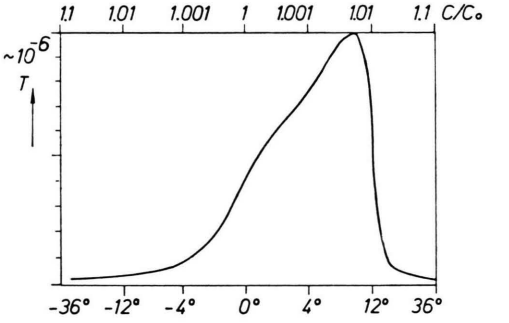

Fig. 6b. Light transmission of a bimolecular film as a function of bulging. The light transmission is normalized to the intensity which enters the torus. The transmitted intensity is measured at the end of a fiber (lenght 120 mm). θ is calculated from the capacitance, assuming $C(\theta)$ to be proportional to the area of the bimolecular film. The film is prepared from a 2% solution of 1,2-di-iso-stearoyl-3-sn-phosphatidylcholine in n-decane. Electrolyte: $1 \cdot 10^{-3}$ M KCl in water, temperature: 23 °C, film aperture: 2 mm.

relative to the separator plane. Excessive bulging or bulging to the reversed direction leads out of the acceptance interval of the film. The half width of the transmission peak of 7 degrees is considerably broader than expected on the basis of the numerical aperture of the fibers. This is attributed to a gradually smoothing transition in the bending radius at the fiber-torus interface. The degeneration of the light transmission due ot the curvature is negligible. For a thickness of the film of 1% of the wavelength the bending radius doubling the forward loss of the plane film is around 10,000 λ [17, 18], whereas the

bending radius at maximum transmission ($\theta = 4.8°$) is 12 mm (24,000 λ).

The background intensity resulting from unguided light — measured in the absence of a film — is 40 times smaller than the peak transmission of $\approx 1 \cdot 10^{-6}$. The bulged film configuration is best suited for transmission experiments since the background intensity is very small contrary to the plane film where guided and background intensity are of the same magnitude. The plane film geometry is useful for scattering experiments with heterodyne detection since the directly transmitted unguided light and the forward scattered light are emitted from the same source with a small spatial angle. This yields a large coherence area necessary for optimum signal to noise ratios in coherent mixing techniques [19].

Applications of Light Guide Effects

The central wave carries predominantly information on the interaction of lipid material with light whereas the surface waves are preferentially modulated by the electrolyte. Since the two waves are coupled, the specific modulation of each wave is taken over by the other one. A separation between the two modulations can be achieved by perturbing either the bilayer or the electrolyte with respect to the light propagation. The application of an electric field is a selective and easily manageable external parameter because the potential drops almost entirely across the bilayer, and the electric field can be modulated in order to meat the requirements for electronic correlation techniques.

The light guide effect is used to investigate the influence of an external electric field on the shape and the structure of a lipid film. The discussion will be concentrated on electrostrictive effects, their detection and identification on the basis of their time constants.

A dc rectangular voltage pulse of 120 mV and 100 ms duration is applied to the lipid film bulged to its maximum transmission. 50 runs are averaged with the WP 2221 system. The transmitted intensity is normalized to the intensity measured at zero electric field. In Fig. 7a the transmission decreases by 18% upon application of the voltage pulse. The transmitted intensity is decaying with a time constant of 16 ms when the voltage is turned on, and recovers with a time constant of 33 ms when the electric field is switched off. An identical response is observed if an ac-instead of a dc-voltage pulse is applied (dotted line). This gives evidence that the transmitted light is modulated by a square law effect independent of the sign of the electric field.

The relatively long time constant suggests that the torus transition region is involved in this effect where a voltage dependent transport of material between the torus and the bilayer has been observed with the capacitance technique [20]. The modulation arises from voltage induced changes of the profile of the torus in its function as a horn shaped coupling element. With the application of an electric field the contact angle γ between the torus and bilayer increases and the length of the transition region is reduced. According to [5, 12] the essential contributions of a field induced change in shape are expected to originate from the torus transition zone, where the thickness decreases from 5000 Å to

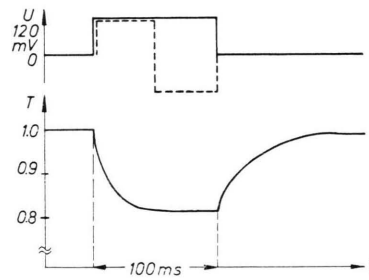

Fig. 7a. Modulation of the transmitted light by an electric field. Upper trace: 100 ms voltage pulse, ± 120 mV amplitude, lower trace: response of the transmitted intensity to the voltage pulse. 50 runs are averaged with a WP 2221 Signal Processing system. The modulation signal is independent of the polarity of the exciting voltage pulse. The other experimental conditions correspond to those in Figure 6b.

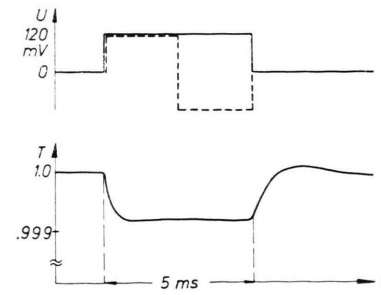

Fig. 7b. Modulation of the transmitted light by an electric field displayed on a shorter time scale. Upper trace: 5 ms voltage pulse, amplitude of ± 120 mV, lower trace: response of the transmitted intensity. The other experimental details are identical with those in Figure 7a.

the bimolecular dimensions of approximately 50 Å. The theory of tapered couplers [13] predicts that this torus section critically determines the light coupling properties of the whole coupler. The coupling efficiency is degraded with a larger contact angle and a shorter transition region.

The torus transition region has been identified as the origin of the light modulation by a different transmission experiment using a prepared separator foil. This allowed to guide the light exclusively inside the torus transition region, i.e. along a secant close to the rim of the aperture. Identical time constants were observed, but the modulation ratio was greatly enhanced (90%). This additional component of the modulation, which only occurs when the light is guided through the torus transition region, is due to thickness dependent mode changes of a wave guide. With an initial thickness, which is comparable or greater than the wavelength of the light, the torus can support propagation modes of higher order and more intensity can be transmitted between the fibers. A reduction in the torus thickness to a fraction of λ cuts off all the higher modes, thereby reducing the transmitted intensity. Thus, the time constants of the transmitted light intensity monitors the displacement of the lipid material in the torus transition region.

A different effect with square law characteristic can be observed on a shorter time scale. Figure 7b shows the change of transmission upon a dc and ac voltage pulse of ± 120 mV amplitude and 5 ms duration after averaging 50 runs. A modulation with an amplitude of $8 \cdot 10^{-4}$, normalized to zero field, is observed decaying with 210 μs time constant and recovering with 260 μs. This effect originates from the bilayer portion of the lipid film since the observed amplitude of modulation is proportional to the light path within the bimolecular area. Under the electric pressure the bimolecular film is supposed to be uniformly or inhomogeneously compressed by squeezing the solvent into microlenses [21]. Because the time constants of the torus and bilayer effects differ by a factor of hundred, the torus remains unchanged during the observation of the bimolecular effects.

A simple compression of the bilayer in thickness would give no net effect in the transmitted light; only some light intensity carried by the center wave would then be shifted to the surface wave not affecting the total intensity. Thus, the observed effect is explained by an inhomogeneous compression of the film during which the solventd is squeeze into microlenses.

As working hypothesis the lenses are assumed to be the scattering centers. Upon application of an external field these centers are generated, or, if permanently existent, change their shape thereby increasing light scattering. The wave guide becomes turbid since a fraction of the guided light intensity is scattered in all directions. The ratio of transmitted intensities with and without field can be expressed by an exponential law:

$$I_{\text{field}}/I_{\text{no field}} = e^{-\tau l}, \tag{19}$$

where τ is the field generated turbidity and l the optical path length within the bilayer. With the help of some simplifying assumptions, the standard formula for intensity scattering experiments can be applied which relates the turbidity to the concentrations and average molecular weight of the scattering centers [22]:

$$\tau = g\,\mu \frac{32\pi^3 N^2}{3 L \lambda^4} \left(\frac{\mathrm{d}n_2}{\mathrm{d}g}\right)^2; \tag{20}$$

g concentration, μ average molecular weight of the scattering centers, L Avogadros number, $\mathrm{d}n_2/\mathrm{d}g \approx 0.19$ cm³/g concentration increment.

By measuring the turbidity at different wavelengths, the product $g\mu$ can be determined and if the results reflect the λ^{-4} power law, the following simplifications are justified:

a) The physical dimensions of the scatterers are considerably smaller than the wavelength of the light and the centers are uncorrelated in position. The last statement must be judged with some scepticism since all centers are bound and oriented by the bilayer.

b) The scattering centers are clusters of the solvent (*n*-decane).

c) An average molecular weight μ is attributed to these clusters which is equal to the product of molecular weight and number of the molecules

Figure 8 shows the experimental results of the wavelength dependence of the turbidity τ. In the long wavelength range (6700—4700 Å) the results agree well with the predicted λ^{-4} dependence according to (20). This proves for the first time in

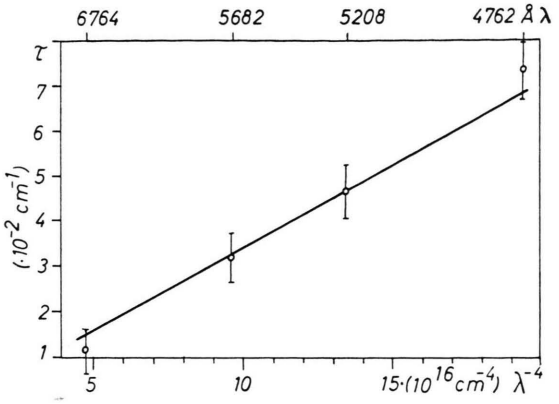

Fig. 8. Dependence of the turbidity induced by an electric field of 120 mV on the inverse of the fourth power of the wavelength (λ^{-4}) transmitted along the bilayer.

an optical experiment the field generation of scattering centers. In the solvent containing film under investigation these centers are attributed to lenses. Since only the product $g\mu = 2.2 \cdot 10^3$ g²/cm³ can be deduced from the slope, information on either the concentration of scattering centers, g, or of the molecular weight of the scattering centers, μ, is necessary. In future experiments the physical dimensions and shape of the scattering centers will be determined via the angular dependence of the scattered light by evaluation of the form factors of the Rayleigh-Debye scattering [23]. These data together with the above simplification (c) allow to calculate the molecular weight of the scattering centers. An appropriate experimental approach may consist in scanning the intensity scattered into the electrolyte by an optical fiber of small numerical aperture. The intensity scattered within the plane of the bilayer can be observed by a set of fibers radially mounted around the aperture.

Conclusions

Lipid bilayers between two aqueous electrolytes exhibit light guiding properties as proven by the transmission of light along a curved path in a bulged film.

These properties are used in transmission and scattering experiments investigating the influence of an electric field on the shape and structure of a lipid membrane.

The external field changes the shape of the transition region between torus and bilayer thereby affecting the transition zone in its function as light coupling element. This leads to a modulation of the transmitted intensity. In the bimolecular area the electric field induces the formation of scattering centers giving rise to an increase of the optical turbidity due to Rayleigh-scattering. The typical λ^{-4} dependence in wavelength is observed for intensity scattering. The scattering centers are tentatively attributed to solvent containing lenses.

By combining the light guide method with dynamic light scattering techniques (light beating spectroscopy) several fundamental properties of the lipid bilayer can be studied like relaxation, drift and diffusion processes as well as conformational changes and equilibrium fluctuations.

Acknowledgements

We are highly indebted to Professor W. Helfrich, Berlin, for constructive and stimulating discussions.

Financial support from the Deutsche Forschungsgemeinschaft is gratefully acknowledged.

[1] P. Mueller, D. O. Rudin, H. T. Tien, and W. G. Wescott, Nature London **194**, 979 (1962).
[2] P. Läuger and E. Neumcke, Membranes – a Series of Advances, Ed. G. Eisenmann, Vol. II, p. 1, Marcel Dekker, New York 1973.
[3] D. F. Sargent, J. Membrane Biol. **23**, 227 (1975).
[4] R. Benz, P. Läuger, J. Membrane Biol. **27**, 171 (1976).
[5] J. Requena and D. A. Haydon, J. Colloid Interface Sci. **51**, 315 (1975).
[6] H. P. Braun and M. E. Michel-Beyerle, Z. Naturforsch. **33a**, 1594 (1978).
[7] M. Montal and P. Mueller, Proc. Nat. Acad. Sci. **69**, 3561 (1972).
[8] R. C. Waldbillig and G. Szabo, Biochem. Biophys. Acta **1979**, in press.
[9] J. Kane and H. Osterberg, J. Opt. Soc. Amer. **54**, 347 (1964).
[10] J. D. Swalen, M. Tacke, R. Santo, K. E. Rieckhoff, and J. Fischer, Helv. Chim. Acta **61**, 960 (1978).
[11] J. N. Polky and J. H. Harris, J. Opt. Soc. Amer. **62**, 1081 (1972).
[12] S. H. White, Biophys. J. **12**, 432 (1972).
[13] D. Marcuse, Bell. Syst. Techn. J. **50**, 273 (1970).
[14] R. K. Winn and J. H. Harris, IEEE Trans. Microwave Theory and Tech. MTT **23**, 92 (1975).
[15] N. S. Kapany and S. Narinder, Dielectric Wave Guides, Academic Press, London 1972.
[16] M. E. Johnson, S. Simon, J. W. Kauffman, and R. C. MacDonald, Biochem. Biophys. Acta **291**, 587 (1973).
[17] E. A. J. Marcatili, Bell. Syst. Techn. J. **48**, 2103 (1969).
[18] L. Levin, IEEE Trans. Microwave Theory and Techn. MTT **22**, 718 (1974).

[19] J. B. Berne and R. Pecora, Dynamic Light Scattering, John Wiley, New York 1976.
[20] J. M. Crowley, Biophys. J. **13**, 711 (1973).
[21] J. Requena, D. A. Haydon, and S. B. Hladcky, Biophys. J. **15**, 77 (1975).
[22] G. Oster, Techniques of Chemistry, Vol. I, Physical Methods of Chemistry, Part III A, Eds. A. Weissberger and B. Rossiter, p. 75, John Wiley, New York 1972.
[23] P. Latimer and P. Barber, J. Colloid. Interface Sci. **63**, 310 (1978).